Kinetics and Catalysis, Vol. 45, No. 5, 2004, pp. 694–701. Translated from Kinetika i Kataliz, Vol. 45, No. 5, 2004, pp. 734–741.

Anomalous Phenomena in Oxygen Desorption from Tungsten and Their Mathematical Modeling

V. V. Savkin, V. Yu. Bychkov, and M. U. Kislyuk

Semenov Institute of Chemical Physics, Russian Academy of Sciences, Moscow, 117977 Russia

Received April 24, 2003

Abstract—A model is developed that describes unusual phenomena in oxygen desorption from tungsten surfaces: (1) in temperature-programmed desorption (TPD) in the transfer from the linear regime of sample heating to the isothermal regime, a maximum of the desorption rate is observed; (2) in the stepped partial desorption of oxygen, the beginning of each subsequent TPD peak shifted toward higher temperatures; (3) the apparent activation energy of desorption increased in the latter case by a factor of ~3 (from 280 to 920 kJ/mol). Monte Carlo modeling that takes into account surface migration of adsorbed oxygen atoms and their lateral interactions gave semiquantitative description of experimental data.

INTRODUCTION

When describing desorption of gases, Langmuir's assumption of an ideal adsorption layer and the derivative kinetic surface action law are used. The rate of desorption w_{des} is described by the equation

$$w_{des} = -d\theta/dt = k^0_{des}\theta^q \exp(-E_{des}/RT), \quad (1)$$

where θ is the fraction of the surface occupied by the adsorbate, $k^0_{des}\exp(-E_{des}/RT)$ is the rate constant of desorption, q is the kinetic order of desorption, R is the universal gas constant, and T is the surface temperature.

This equation at a constant temperature (T) and any positive q describes a monotonically decreasing dependence of the rate of desorption on time.

In the 1980s, some papers [1–4] reported a maximum in the isothermic desorption rate that cannot be explained by Eq. (1). The authors of [1, 2] explain the appearance of maximums in the rate of isothermal desorption by the attractive lateral interactions between adsorbed species due to which the rate constant of desorption is the function of the surface concentration of adsorbates:

$$k_{des} = k^0_{des}\exp[-(E_0 + A\theta)/RT], \quad (2)$$

where E_0 is the activation energy of desorption of the isolated species and A is the coefficient that characterizes the effect of θ on the activation energy of desorption.

Of course, this macroscopic approach can explain the maximum of the desorption rate at a constant temperature, as shown in [1, 2]. However, this model is rather rough, since it considers the averaged concentration of an adsorbate. Under real conditions, the attractions of adsorbed molecules or atoms lead to the formation of adsorbate islands, and local concentrations may differ substantially.

In this work we use a microscopic approach based on Monte Carlo modeling of the process to describe anomalous oxygen desorption from tungsten that was observed in [3, 4]. In desorption modeling, we took into account the lateral interaction in the adsorption layer and the surface migration of adsorbed oxygen atoms. The latter occurs at a much higher rate than desorption because the ratio of the activation energies of desorption and migration is $E_{des}/E_{mig} \approx 3$ [5].

Anomalous Phenomena in Oxygen Desorption from Tungsten

The O/W system is one of the few systems in which oxygen desorption is atomic [6]. The desorption of atomic oxygen is preceded by the desorption of the tungsten oxides from the surface at lower temperatures (WO, WO_2, and WO_3) [7].

Figure 1 shows the dependences of the rate of temperature-programmed desorption (TPD) of atomic oxygen observed after its adsorption on polycrystalline tungsten at room temperature and various exposures [3]. As can be seen from this figure, broad peaks with maximums at ~2000 K are observed in all cases. In this work, oxygen coverages (θ) were recalculated because of data reported in [7], according to which only 75% of oxygen desorption from the saturated layer is atomic. The parameters of the rate constants calculated based on the analysis of desorption peaks are as follows: the activation energy is $E_{des} = 310 \pm 50$ kJ/mol and $k^0_{des} = 10^7$–10^9 s^{-1}. The value k^0_{des} is thus strongly underestimated compared to the theoretical value (10^{12}–10^{13} s^{-1}).

The most pronounced deviation from the classical kinetics of desorption was observed in TPD experiments with a transition from the linear heating rate of the sample to the isothermal regime [3], as Figure 2

0023-1584/04/4505-0694 © 2004 MAIK "Nauka/Interperiodica"

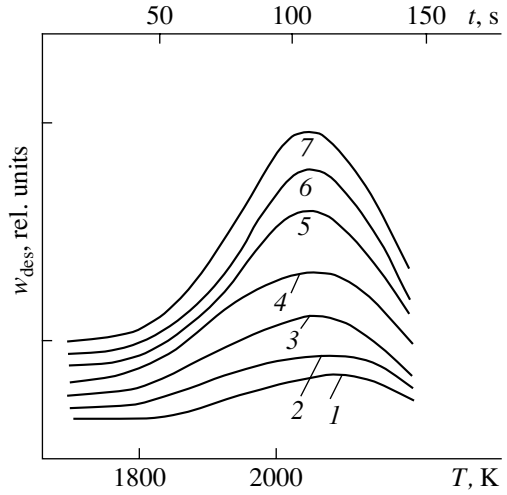

Fig. 1. Experimental TPD spectra of oxygen adsorbed on tungsten at 300 K and various exposures initial coverages θ_0 [3]: (*1*) 0.14, (*2*) 0.17, (*3*) 0.24, (*4*) 0.35, (*5*) 0.53, (*6*) 0.62, and (*7*) 0.70.

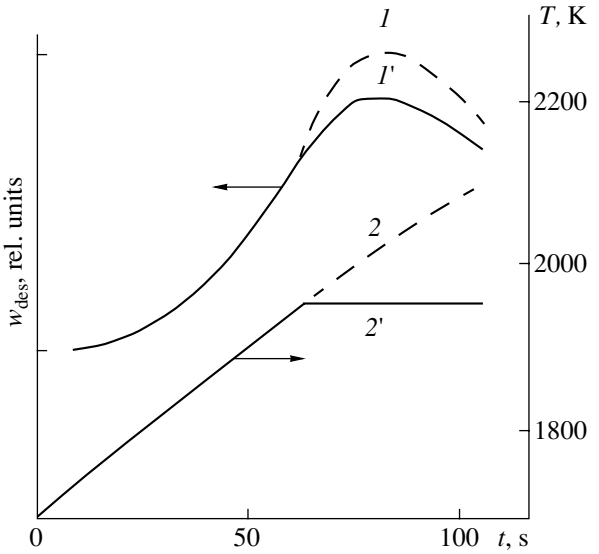

Fig. 2. Experimental dependences of the rate of oxygen desorption from tungsten on time [3] ($\theta_0 = 0.7$) in the case of (*1*) the linear growth of temperature and (*1′*) in the transfer from the regime of linear heating to isothermal and (*2, 2′*) the corresponding dependences on temperature.

illustrates. It can be seen that, with a transfer to the isothermal regime, the rate of desorption continues to increase and then passes through a maximum. In contrast to data reported in [1, 2], for oxygen on platinum and nitrogen on tungsten this transfer does not lead to a noticeable break in the kinetic curves.

Figure 3 demonstrates the results of TPD experiments [4] in which various surface concentrations of oxygen were obtained after one or several cycles of heating, keeping at a constant temperature, and cooling the sample with a preadsorbed saturated layer of oxygen. Arrows show instants corresponding to the transition to the isothermal heating of the sample. For comparison, we show the kinetic curve of oxygen desorption rate from the saturated layer.

These results differ substantially from those shown in Fig. 1. Here with a decrease in the surface concentration of oxygen, we observe a significant consecutive shift (to 200 K) of the kinetic curves toward higher temperatures. As a result, the value of the apparent activation energy increases from 280 to 920 kJ/mol (Fig. 4).

Thus, the deviation of the kinetics of atomic oxygen desorption from tungsten from the classical variant reveals itself in the following features:

(1) The TPD peak of oxygen is substantially broadened, which can point to the low value of the preexponential factor of the apparent rate of desorption compared to the theoretical one.

(2) In the broad range of temperatures and surface concentrations, isothermal maximums of the desorption rate are observed.

(3) The apparent activation energy of desorption depends on the way the adsorption layer is formed. If the exposure varies, it remains constant within the experimental error. In the same range of coverages obtained due to partial oxygen desorption from the saturated layer, a considerable increase in the apparent activation energy of desorption is observed along with a decrease in its surface concentration.

Only the first of these main results can be considered trivial. To explain each of these separately, one can propose one or several models.

TPD peak broadening can be due to the nonuniformity of the surface [8], lateral repulsion of adsorbates [9], or desorption through the precursor state [10].

The isothermal maximums of the desorption rate can be explained by the consecutive processes, and by the attraction of the adsorbed species to each other [1–3]. Lateral attraction may lead to the formation of adsorbate islands, in which desorption largely occurs from island boundaries [3].

Although an increase in the apparent activation energy of desorption with a decrease in θ can quantitatively be described by surface nonuniformity or lateral interactions, the absolute value of the change from 280 to 920 kJ/mol is hard to explain using these factors.

CHOICE OF THE MODEL AND ITS DESCRIPTION

The main requirement on the model is that it should be able to describe all three experimental results listed above. Therefore, we reject schemes that did not meet this requirement. We also exclude models that are based on the idea of surface nonuniformity and an accounting

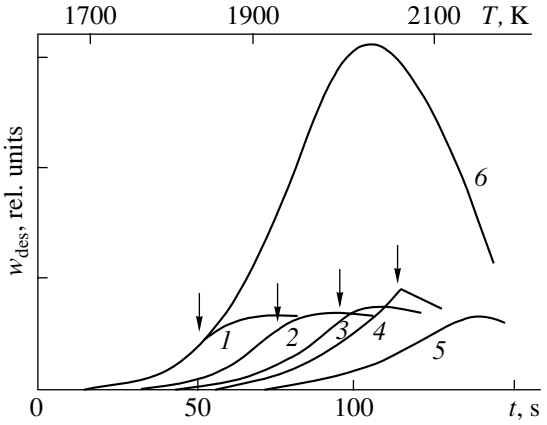

Fig. 3. TPD spectra of the samples with a preadsorbed oxygen layer obtained in the consecutive 1–5 cycles of heating, keeping at a constant temperature and cooling (curves *1–5*, respectively) [4]. Arrows shows the transition to the isothermal regime. (*6*) TPD spectrum corresponding to curve *7* in Fig. 1.

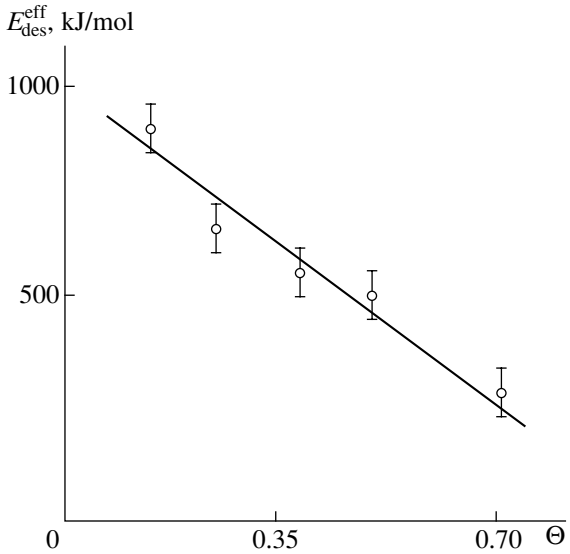

Fig. 4. Dependence of the apparent activation energy of oxygen atom desorption calculated in [4] from the initial portions of curves in Fig. 3.

for lateral interactions according to Eq. (2). The first does not describe the isothermal maximums of the desorption rate, and the second fails to explain even qualitatively the effects shown in Figs. 1, 3, and 4.

Earlier we proposed a model [3] that takes into account the attractive lateral interactions of adsorbate species, which results in the formation of close-packed islands of the adsorbed phase. The consideration of lateral interactions, which are 3–8 kJ/mol in strength for oxygen on tungsten [11], results in a situation in which atomic oxygen desorption occurs more readily if an atom has fewer neighbors. This model allow us to qualitatively explain all the observed anomalous effects.

In this work, we use Monte Carlo methods for quantitative modeling of the observed effects. We assume that the tungsten surface largely consists of the closed-packed bbc W(110) face shown in Fig. 5.

In our model, we used a 100×100 lattice in the form of a parallelogram. To avoid boundary effects, the opposite sides of the lattice were "sewn together." Each active site of the surface can be vacant or occupied by an adsorbed oxygen atom.

Each adsorbed atom experiences attractions of neighboring oxygen atoms, the number of which ranges from one to six. For simplicity of calculations, all six nearest neighbor sites were considered equivalent, although the structure of the W(110) plane is somewhat different from the hexagonal plane, as shown in Fig. 5.

The adsorbed atom may desorb or migrate to the neighboring vacant active site on the surface.

The probabilities of desorption (P_{des}) and migration (P_{mig}) of atoms per unit time were defined by the equations:

$$P_{des} = k_{des}^0 \exp[-E_{des}(n)/RT], \quad (3)$$

$$P_{mig} = (6 - n) k_{mig}^0 \exp[-E_{mig}(n)/RT], \quad (4)$$

where k_{des}^0 and k_{mig}^0 are the preexponential factors of the rate constants of desorption and migration (s^{-1}), $E_{des}(n)$ and $E_{mig}(n)$ are the activation energies (kJ/mol) depending on the number (n) of occupied neighboring sites, and T (K) is the current temperature.

By modeling the two-center dissociative adsorption of O_2 on the hexagonal lattice, we determine the maximal coverage by oxygen atoms: 0.92–0.93 ML. It was shown in [7] that, in TPD of oxygen from the saturated layer on tungsten, only 75% of oxygen desorbs in the atomic state. The rest of oxygen desorbs in the form of tungsten oxides at lower temperatures. In connection with this, we modeled the period starting from when the initial surface coverage by oxygen atoms was equal to ≤0.7 ML, at which point adsorbed oxygen atoms were randomly distributed over the surface.

The computer code that we developed enables us to use a model of a linear temperature increase with time (a model of temperature-programmed desorption) and a constant-temperature model (a model of isothermal experiment), as well as to alter these regimes.

The process of modeling consists of step-by-step computation in time taking into account the rate constants of desorption and migration. At each step the overall probability of all possible events (desorption and migration of atoms) is calculated using Eqs. (3) and

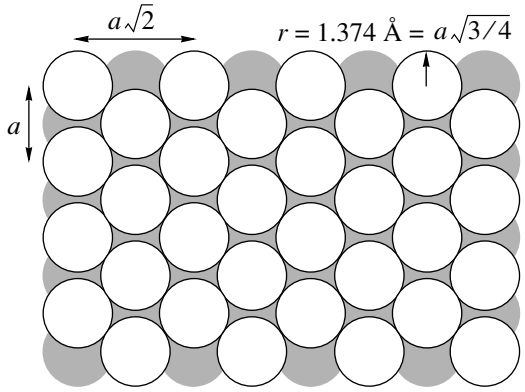

Fig. 5. The structure of the bcc W(110) face; r is the radius of a tungsten atom, and a is the lattice constant.

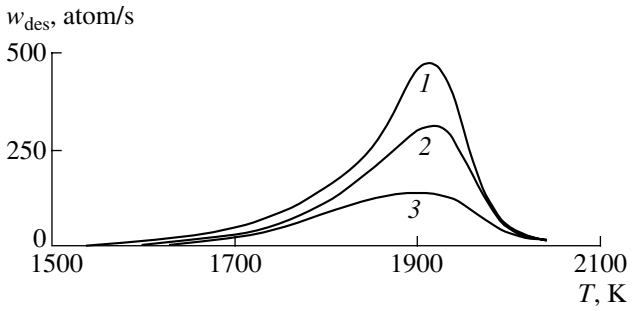

Fig. 6. Simulated TPD spectra of oxygen on the tungsten 100 × 100 lattice. The initial coverage θ_0: (*1*) 0.7, (*2*) 0.5, and (*3*) 0.3.

(4) per unit time and the time period for which this probability is equal to unity.

Then, a random number from the range (0, 1) was generated, and it was determined to which event's probability range it belonged to. If the chosen event was atom migration and the number of neighboring vacant sites was greater than unity, then the specific direction of migration was taken at random. If there was only one vacancy near the chosen atom, then the atom moved to this vacant site.

After a corresponding change in the distribution of atoms over the surface, this cycle is repeated until the final time or temperature was reached.

The results of modeling were the snapshots showing the distributions of vacant and occupied sites and the dependences of the rate of desorption on time or temperature.

The rate of desorption was calculated as follows. From some moment in time, the number of desorbed atoms was counted. When this number reached a certain value (usually 30), this number was divided by the time period, and thus the average rate of desorption during this period was obtained.

Variables in the modeling were as follows: the preexponential factors and the activation energy of desorption and migration of an isolated (having no nearest neighbors) adsorbed oxygen atom, and the value of the lateral interaction of an oxygen atom with its nearest neighbors. The latter was chosen from the range 3–8 kJ/mol, based on the results reported [11].

The dependences of $E_{des}(n)$, which are involved in Eqs. (3) and (4), were approximated by monotonically increasing the functions of the n nearest adsorbed oxygen atoms. The form of these functions was varied for the optimal description of experimental results. The best approximation of experimental results was obtained for the following values of variables: k^0_{des} = 10^6 s^{-1}, $E_{des}(n)$ = 240 (n = 0), 242 (1), 247 (2), 259 (3), 272 (4), 280 (5), and 282 (6) kJ/mol. The average value of the energy of lateral interaction per one neighboring oxygen atom was at most 8 kJ/mol. This value agrees with the results reported in [11].

According to experimental data on the diffusion coefficients for oxygen on tungsten [12–16], the ratio E_{des}/E_{mig} ranges from 2 to 4.

In [16], based on data reported in [12–16], we obtained a correlation of the diffusion coefficient (D) for oxygen on tungsten and temperature in a wide temperature range (400–1500 K). In the coordinates of the Arrhenius equation, all the above data fit well the same straight line corresponding to the preexponential factor of the diffusion coefficient $D_0 \approx 10^{-2}$ cm^2/s.

The relationship between the rate constant of migration (k_{mig}) and the diffusion coefficient in the presence of interaction between adsorbed species was defined by the formula [5]

$$D = (\lambda^2 k_{mig})/4, \quad (5)$$

where λ is the average length of a hop of the adsorbed species, which was assumed to be equal to the average distance between neighboring active sites (tungsten atoms). For the bbc W(110) face, this value is 2.88 Å.

The substitution of the numerical values of the parameters in Eq. (5) gives us the value of the preexponential factor of the rate constant of migration $k^0_{mig} = 5 \times 10^{13}$ s^{-1}, which completely agrees with the absolute rate theory.

The dependence $E_{mig}(n)$ was constructed while taking into account a simple relationship:

$$E_{mig}(n) = E_{mig}(0) + \Delta_n E, \quad (6)$$

where $E_{mig}(0)$ is the activation energy of migration of an isolated oxygen atom and $\Delta_n E$ is the energy of lateral interaction of oxygen with its n nearest neighbors. The values $\Delta_n E$ were assumed to be the same as for the dependence of $E_{des}(n)$.

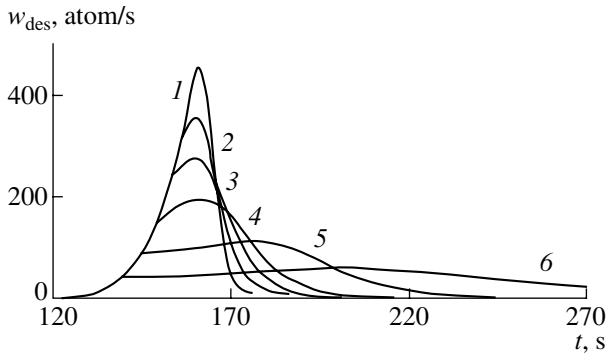

Fig. 7. Simulated TPD spectra of oxygen on tungsten at $\theta_0 = 0.7$. Curve 1 corresponds to continuous linear heating of the sample. Curves *2–6* were obtained for the case of the transfer of linear heating to the isothermal regime at T, K: (*2*) 1860, (*3*) 1830, (*4*) 1800, (*5*) 1750, and (*6*) 1700.

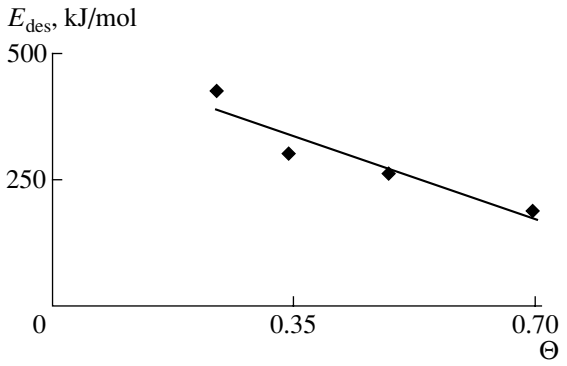

Fig. 9. Dependence of the apparent activation energy of desorption on the surface coverage calculated from the initial portions of the kinetic curves *2–5* in Fig. 8.

Experimental results were best approximated for the following values of the variable parameters: $k^0_{mig} = 10^{13}$ s^{-1}, $E_{mig}(n) = 65$ ($n = 0$), 67 (1), 72 (2), 84 (3), 97 (4), and 105 (5) kJ/mol. For $n = 6$, we assumed that the migration does not occur because of the absence of vacancies in the nearest neighborhood of the adsorbed oxygen atom.

RESULTS OF MATHEMATICAL MODELING

Figures 6–9 show the results of simulations that correspond to the experimental data that are presented in Figs. 1–4. A comparison of Figs. 6 and 1 shows that the temperatures of the maximums of TPD peaks differ within 5% error and are independent of the initial concentration of adsorbed oxygen, in agreement with experimental data. The half-width of experimental and simulated peaks differs somewhat more broadly: 150–200 K (Fig. 1) and 120–200 K (Fig. 6). This difference is probably due to the deviation of the experimental temperature from the linear law, whereas temperature increased strictly linearly in simulations.

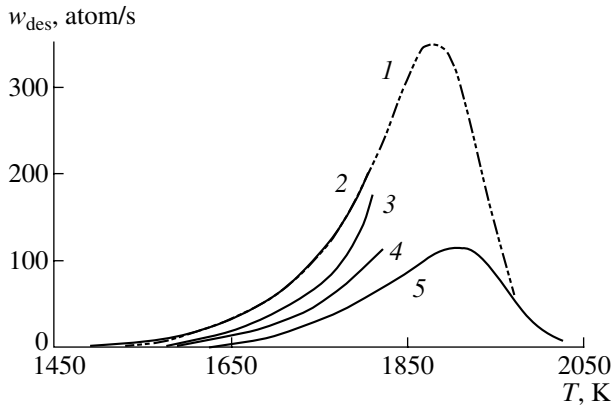

Fig. 8. The results of modeling the shift of the consecutive kinetic curves toward higher temperatures corresponding to experiments in Fig. 3. Solid lines correspond to the coverages θ_0: (*2*) 0.6, (*3*) 0.4, (*4*) 0.3, and (*5*) 0.2. Dashed line *1* was obtained by the simulation of uninterrupted linear heating of the sample with the preadsorbed oxygen layer ($\theta = 0.6$).

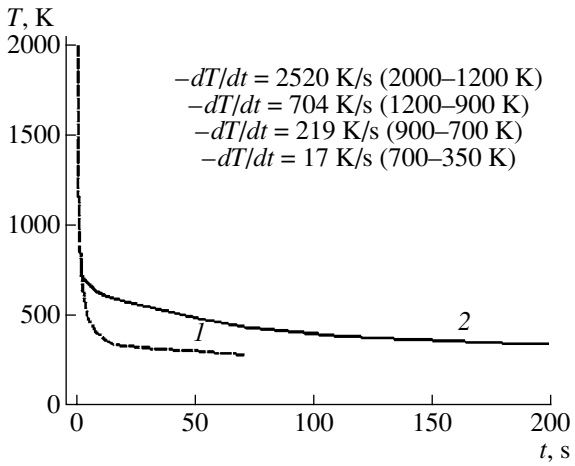

Fig. 10. Kinetic curves of sample cooling (*1*) calculated by numeric integration of Eq. (7) and (*2*) taking into account the temperature of current leads (see text). The average rates of cooling in the mentioned temperature range are shown at the top.

The model gives quite an acceptable description (Fig. 7) of the experimental isothermal maximums of the desorption rate (Fig. 2), and there is no noticeable break in the kinetic curves in the transfer from the regime of linear heating to the isothermal high-temperature regime, also in agreement with the experiment.

In the simulation of experiments in the regime of heating–cooling of the samples (Fig. 3), it was necessary to know the rate of sample cooling. The sample temperature, after its heating has been interrupted, does not decrease instantaneously, as can be seen by its luminance.

When heating is discontinued, the desorption of oxygen atoms discontinues rather rapidly, due to the high activation energy of this process. However, the

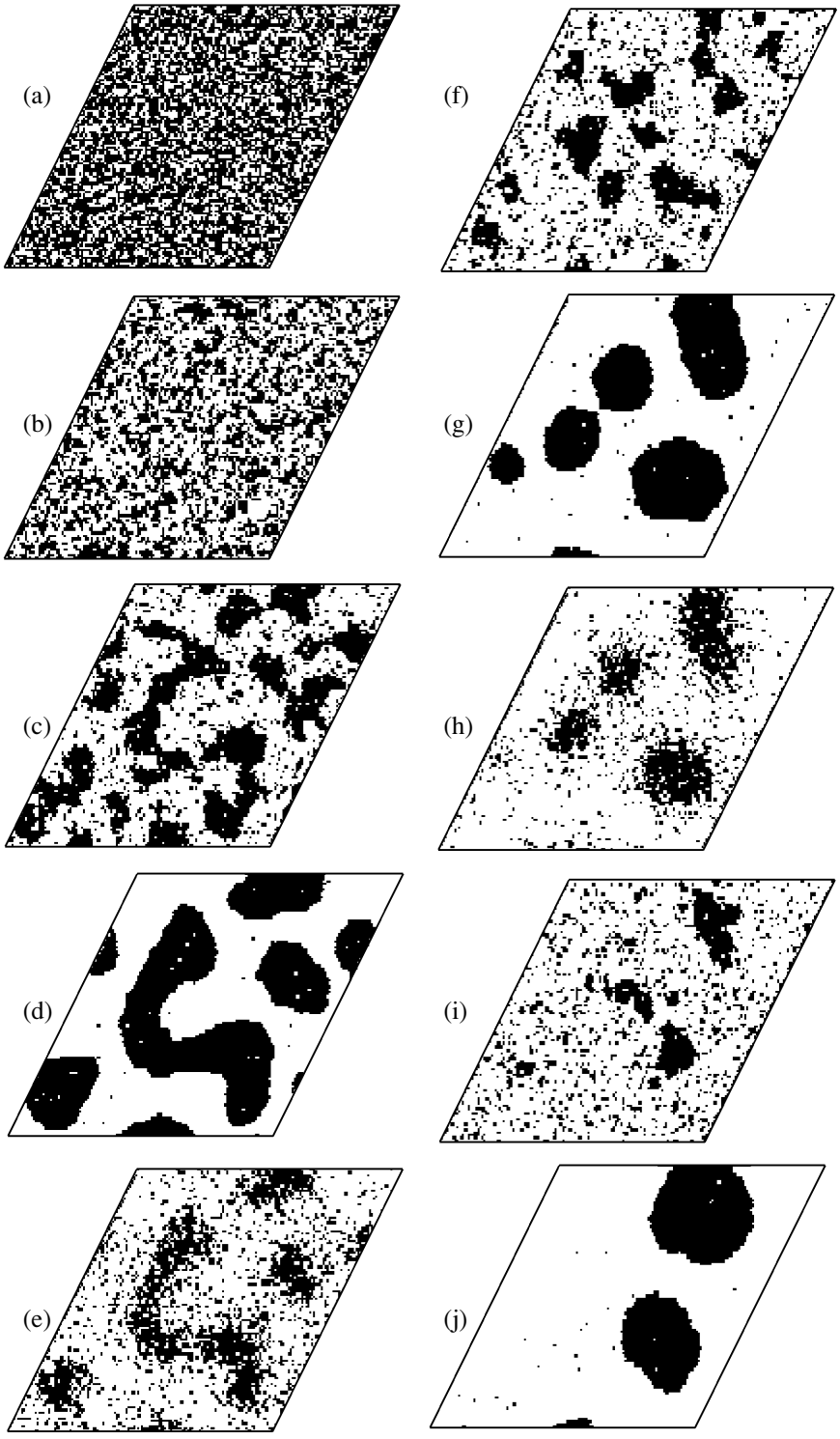

Fig. 11. Evolution of the distribution of adsorbed oxygen atoms on the surface in the modeling of the consecutive cycles of heating and cooling: (a) initial statistical distribution at $\theta_0 = 0.6$; (b) heating to 1770 K (desorption) ($\theta = 0.4$); (c) cooling to 1000 K ($\theta = 0.4$); (d) cooling to 400 K ($\theta = 0.4$); (e) heating to 1775 K (desorption) ($\theta = 0.3$); (f) cooling to 1000 K ($\theta = 0.3$); (g) cooling to 400 K ($\theta = 0.3$); (h) heating to 1880 K (desorption) ($\theta = 0.2$); (i) cooling to 1000 K ($\theta = 0.2$); and (j) cooling to 400 K ($\theta = 0.2$).

surface migration of oxygen is very fast even at low temperatures.

As we will show below, with a decrease in temperature, the process of migration leads to the structuring of the adsorption layer in the form of a two-dimensional condensation of the adsorbed layer.

Because the sample was in a vacuum, we assumed that its cooling upon switching the heat off is largely

due to thermal radiation. Therefore, the rate of cooling was calculated using the Stefan–Boltzmann equation

$$Q = \alpha\sigma T^4,$$

in which Q is the rate of thermal energy loss from the unit surface area, T is the absolute temperature of the surface, $\sigma = 5.75 \times 10^{-5}$ erg cm^{-2} s^{-1} deg^{-4} [18] is the Stefan coefficient for an absolute black body, and α is the average coefficient of radiation.

Taking into account the specific heat capacity of tungsten $c = 24.02 + 0.01T$ J mol^{-1} deg^{-1} [17], $\alpha = 0.45$ [18], the sample size $50 \times 3 \times 0.025$ mm, and its density $\rho = 19.3$ g/cm^3 [18], the Stefan–Boltzmann equation can be written in the following form:

$$-dT/dt = S\alpha\sigma(T^4 - T_{room}^4)/c\rho V, \quad (7)$$

where S and V are the surface area of the sample and its volume, and T_{room} is room temperature.

Taking into account the values of all parameters in Eq. (7), we numerically integrated this equation. The resulting dependence of temperature on time is shown in Fig. 10 by a dashed line. The sample in the form of a tungsten strip was soldered to bulk molybdenum rods (current leads), whose temperature is increased to 700 K during sample heating. Therefore, its cooling at temperatures below 700 K is slowed down compared to the above curve. The real curve of cooling at $T < 700$ K was shown by a solid line. The curve of temperature lowering was approximated by an open polygon and at each section the average rate of cooling was calculated, which is shown in Fig. 10 for the temperature ranges 2000–1200, 1200–900, 900–700, and 700–350 K. The resulting data were used in the modeling of the cycles of sample heating and cooling.

The results of the modeling are illustrated in Fig. 8. Here, we also obtain adequate results. Specifically, the consecutive kinetic curves moved towards the region of higher temperatures, and all were inside a peak enveloping them and registered in the case of uninterrupted heating of the sample with a preadsorbed oxygen layer ($\theta = 0.6$).

Note that the simulated dependence of the apparent activation energy of desorption on the surface coverage (Fig. 9) gives (as in the experiment; Fig. 4) approximately a threefold increase of its value, with a decrease in θ from 0.6 to 0. However, the simulated absolute values of the activation energy were approximately twice as low as in the experiment.

Such a discrepancy in the absolute values of the apparent activation energy is probably due to the fact that they were obtained from different initial portions of TPD peaks (i.e., at low rates of desorption).

As mentioned above, in the process of modeling we obtain not only the dependence of the rate on time and temperature but also the distribution of adsorbed oxygen atoms on the surface of tungsten.

Figure 11 shows the evolution of these distributions in consecutive cycles of heating and cooling of the surface. The initial coverage of the tungsten surface by oxygen atoms was $\theta = 0.6$. As can be seen from this figure, in the consecutive cycles the adsorbed layer is structured and adsorbate islands grow, while the concentration of isolated oxygen atoms decreases. As a result, a growing number of adsorbed atoms concentrate in close-packed islands with minimal perimeter values. Due to the lateral interactions (attraction) between the nearest neighbors, the desorption of oxygen atoms from these islands is much slower than for the atoms at the island boundaries and for isolated oxygen atoms.

CONCLUSION

The explanation [3] for a set of anomalous phenomena observed in the desorption of oxygen atoms from tungsten was generally confirmed in the modeling of this system by the Monte Carlo method, taking into account lateral interactions of adsorbed atoms and their migration over the surface.

We managed to obtain almost quantitative agreement between model simulations and experimental data using real interaction and surface migration parameters, which are known from published data [5, 11–16].

We plan to modify this model to take into account lateral interactions with more distant neighbors than the nearest ones. One should also include in the model the dissolution of oxygen in the bulk of tungsten oxide formation. This will probably make the description of anomalous phenomena more accurate.

ACKNOWLEDGMENTS

This work was supported by the Russian Foundation for Basic Research (grant no. 02-03-33097). We thank V.V. Sadovnikova for fruitful discussions.

REFERENCES

1. Barteau, M.A., Ko, E.I., and Madix, R.J., *Surf. Sci.*, 1981, vol. 102, no. 1, p. 99.
2. Lee, J., Madix, R.J., Schlaegel, J.E., and Auerbach, D.J., *Surf. Sci.*, 1984, vol. 143, nos. 2–3, p. 626.
3. Savkin, V.V., Kislyuk, M.U., and Sklyarov, A.V., *Kinet. Katal.*, 1988, vol. 29, no. 1, p. 168.
4. Savkin, V.V., Kislyuk, M.U., and Sklyarov, A.V., *Heterogeneous Catalysis: Proc. 6th Int. Symp. in Sofia*, 1987, vol. 2, p. 28.
5. Kislyuk, M.U., *Kinet. Katal.*, 1998, vol. 39, no. 2, p. 246.
6. Ptushinskij, Yu.G. and Chuikov, B.A., *Surf. Sci.*, 1967, vol. 6, no. 1, p. 42.
7. Bauer, E. and Engel, T., *Surf. Sci.*, 1978, vol. 71, no. 3, p. 695.
8. Kislyuk, M.U. and Rozanov, V.V., *Kinet. Katal.*, 1995, vol. 36, no. 1, p. 89.

9. King, D.A., *Chemistry and Physics of Solid Surfaces*, Wanselow, R. and Tong, S.Y., Eds., Boca Raton: CRC, 1979, vol. 2, p. 87.
10. Corte, R. and Schmidt, L.D., *Surf. Sci.*, 1978, vol. 76, no. 3, p. 559.
11. Williams, E.D., Conningham, S.L., and Weinberg, W.H., *J. Chem. Phys.*, 1978, vol. 68, no. 10, p. 4688.
12. Engel, T. and Gomer, R., *J. Chem. Phys.*, 1970, vol. 52, no. 4, p. 1832.
13. Butz, R. and Wagner, H., *Surf. Sci.*, 1977, vol. 63, no. 2, p. 448.
14. Chen, J.-R. and Gomer, R., *Surf. Sci.*, 1979, vol. 79, no. 2, p. 413.
15. Bowker, M. and King, D.A., *Surf. Sci.*, 1980, vol., p. 94.
16. Kislyuk, M.U. and Savkin, V.V., *Kinet. Katal.*, 1986, vol. 27, no. 2, p. 424.
17. *Kratkii spravochnik fiziko-khimicheskikh velichin* (Abridged Handbook of Physicochemical Data), Mishchenko, K.P. and Ravdelya, A.A., Eds., Leningrad: Khimiya, 1972.
18. Kei, D. and Lebi, T., *Spravochnik fizika-eksperimentatora* (A Handbook for an Experimental Physicist), Moscow: Inostrannaya Literatura, 1949, p. 148.